

Study on Dynamic Properties of a Concrete Filled Tubular (CFT) Arch Bridge Constructed in China

by

Qingxiong Wu*, Kazuo Takahashi**, Baochun Chen* and Shozo Nakamura**

The effect of cable loosening on the nonlinear parametric vibrations of inclined cables is discussed in this paper. In order to calculate loosening for inclined cables without a small-sag limitation, it is necessary to first derive equations of motion for an inclined cable. Using these equations and the finite difference method, the effect of cable loosening on the nonlinear parametric responses of inclined cables under periodic support excitation is evaluated. A new technique that takes into account flexural rigidity and damping is proposed as a solution to solve the problem of divergence. The regions that generate compressive forces in inclined cables are also shown.

Key words: concrete filled steel tube, arch bridge, seismic response

1. Introduction

Using CFT (concrete filled steel tubes) for the arch ribs of an arch bridge is rational since CFT is resistant to axial compressive forces. The infilled concrete delays local buckling of the steel tube and the steel tube reinforces the concrete's resistance to tension, bending moments, and shear forces^{1),2)}. The steel tube also acts as a formwork for the concrete during construction of the bridge, thus saving a major construction cost³⁾. Because of these advantages, it is possible to reduce the cost of constructing steel bridges^{4), 5)}. In Japan, the research analysis and experiments of CFT arch bridges have recently been done. The Second Saikai Bridge, which is under construction in Nagasaki Prefecture, is the first CFT arch highway bridge in Japan⁶⁾.

More than 100 CFT arch bridges have been constructed in China since the 1990's and the recent construction technology has been greatly improved. For example, the tubes of the arch ribs are partially filled with concrete, and the arrangement of horizontal steel beams instead of horizontal RC beams is to decrease vehicle-induced vibrations of the main deck. Those technological studies have led to the current construction of a CFT arch bridge with a span of 460m⁷⁾.

The application of the CFT arch bridge is a rational choice in China, where there is only a slight possibility of strong earthquakes occurring. The seismic safety must be carefully checked when the CFT arch bridge is constructed in other countries where strong earthquakes may occur. In Japan, since the Hyogo-ken Nanbu Earthquake, bridges must be ductile and the seismic safety of CFT arch bridges must be verified⁸⁾. The safety of bridges with complex dynamic responses must be checked using two types of ground motions in the Specification for Highway Bridges 1996⁹⁾. The first is the plate-boundary-type earthquakes (Type I) having a magnitude of about 8, and the second is the inland-type earthquakes (Type II) having a magnitude of about 7-7.2 at very short distance. Since the weight of a CFT arch rib is heavier than a steel rib and then the arch action is not effective in the out-of-plane direction, the influence of a large earthquake force in the out-of-plane direction on CFT arch bridges is a concern.

The seismic properties of CFT arch bridges have been the subjects of recent research. Liu et al^{10), 11), 12)} discussed the seismic characteristics of two CFT arch bridges in China and clarified the nonlinear seismic performance of the tentatively designed CFT arch

Received on June 23, 2006

*Department of Civil Engineering, Fuzhou University, China

**Department of Civil Engineering

bridges according to the Japan design standard. Wu et al.¹³⁾ discussed the nonlinear seismic properties of a partially concrete filled steel tubular arch bridge in China and examined the effect of the filled concrete length of steel tube on nonlinear seismic responses of an arch bridge. More studies are necessary in order to fully comprehend the seismic properties of CFT arch bridges.

In this paper, the authors analyze a CFT bridge in China in an attempt to evaluate dynamic characteristics of a CFT arch bridge subjected to strong seismic excitations. This bridge has three spans. The main span of the half-through CFT arch bridge has a span of 251m, which is similar to the length of the Second Saikai Bridge, Japan's first CFT arch highway bridge.

This paper begins by describing the three-dimensional finite element model that is used in the analysis and discussing the natural vibration characteristics of this bridge. A nonlinear seismic analysis is then performed using the strong ground motions recommended in the Design Specification for Highway Bridges 1996⁹⁾. Axial force fluctuation and the non-linearity of the biaxial bending moments of the CFT arch rib are taken into account by using a fiber model. The fine performance of this bridge under strong ground motions is verified. Furthermore, this paper examines the effect of lateral bracing on the nonlinear seismic response of an arch rib since the arrangement of the lateral bracings can be considered as a countermeasure for the out-of-plane seismic responses of the arch bridge. It is concluded that lateral bracings in the quarter span of the CFT bridge may greatly reduce seismic responses.

2. A Brief description of Bridge

The object of the present paper is an arch bridge with three spans that was constructed in China. This bridge is a rigid-frame tied bridge with spans of 60.5 m, 251.0 m and 60.5 m, as shown in Figure 1. The main span is a half-through CFT arch bridge. The side spans are two cantilevered half RC arch bridges. Prestressed steel ties are used to balance the horizontal force in the piers because this bridge is self-balancing. The half-through CFT arch bridge has a 240.0m clear span and a 48.0m clear rise, and the upper-deck RC arch bridges have 55.0 m clear spans and 14.3 m clear rises.

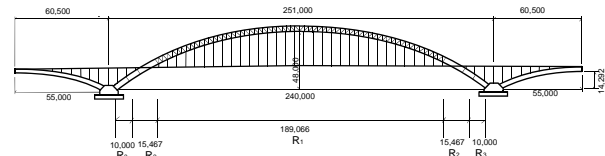


Figure 1 General characteristics of CFT bridge (unit: mm)

The CFT arch rib has three different cross-sections (R1, R2 and R3), as shown in Figure 2. Each of the three cross sections is composed of two horizontal dumbbells. Each dumbbell is comprised of two steel tubes and two plates with a concrete filled inner space. The diameter of the steel tube is 1000 mm and the thickness is 14mm. The steel plate is 800×12mm. The three cross sections differ in the type of connection between the two horizontal dumbbells. The R1 member at the center part of the main span is connected by vertical and diagonal truss tubes. The R2 member is near the joint between the arch rib and the floor system, and the two horizontal dumbbells are connected with web steel plates instead of steel tubes. The inner spaces of the web bars are filled with concrete. The R3 member covers the region starting from the springing part and ending at a horizontal distance of 10 meters. The R3 cross section contains infilled concrete both in the inner span of the web and in the core of the cross section. The reason for filling the inner space with concrete is to prevent collapse of the bridge caused by a collision from a ship passing through under the bridge.

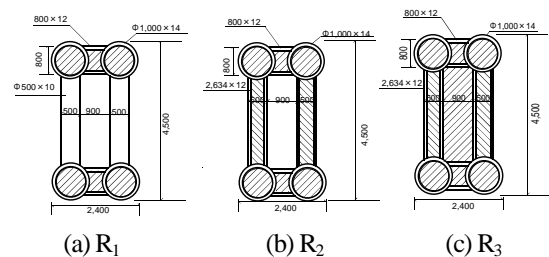


Figure 2 Section of arch rib (unit: mm)

Six K-type lateral bracings, one X-type lateral bracing in the arch rib of the main span, and two K-type lateral bracings in the arch ribs of the side spans are used to ensure the out-of-plane stability of the arch ribs.

3. Analytical model

Figure 3 shows a three-dimensional finite element model of this bridge. Regarding the modeling of the arch rib, the R1 member is modeled using two beam elements, which represent the upper and lower horizontal dumbbells, respectively. In linear analysis, since dumbbells consist of steel tubes and inner concrete, the equaling material property for beam element is calculated using the composite stiffness. The R3 and R2 members, which have concrete filled inner spaces, are considered to be a single member and are modeled using single beam elements.

The column and hanger are modeled using truss elements. The single tie is replaced by two spring elements with equivalent rigidity; these two spring elements are positioned at the two ends of the deck, see S1, S2, S3, and S4 in Figure 3. The stiffness of those springs is set to 1.330 104 kN/m.

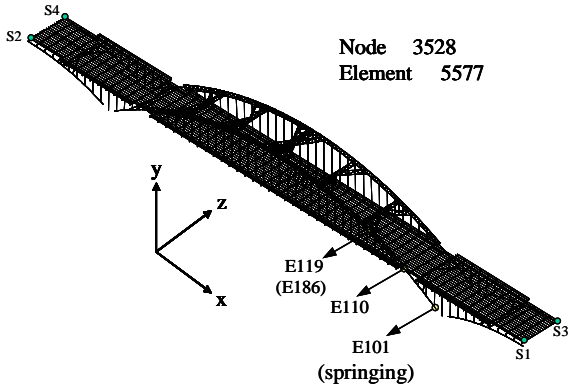




Figure 3 FE model

The following boundary conditions are assumed in this model: (i) all displacements at the end supports of the arch rib are fixed; (ii) the displacement in the longitudinal direction, as well as the rotation around the longitudinal direction, are free at the end supports of the deck, while the other freedoms at the end supports of the deck are constrained.

4. Natural vibration characteristics

The lowest natural frequencies and the corresponding participation factors and modal shapes are shown in Tables 1 and 2.

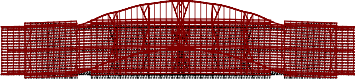
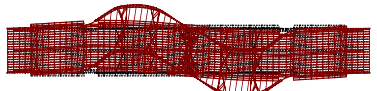
Table 1 Natural modes of in-plane vibrations

No.	Freq. (Hz)	Modal shape
1	0.724	
2	1.229	

The first in-plane vibration is the antisymmetric mode and has a frequency of 0.724 Hz. The second in-plane vibration has a frequency of 1.229 Hz, which corresponds to the symmetric mode of the arch rib.

The first out-of-plane vibration is the symmetric mode and has a frequency of 0.385 Hz, which is lower than the frequency of the first in-plane mode.

Table 2 Natural modes of out-of-plane vibrations

No.	Freq. (Hz)	Modal shape
1	0.385	
2	0.760	

5. Seismic response characteristics

A fiber model is employed in present study in order to evaluate the material non-linearity used for the CFT arch ribs. This model can automatically take into account axial force fluctuation and the non-linearity of the biaxial bending moments. The elastic perfect plastic model is used for the steel tube. The stress-strain curve proposed by Sato [14], which takes into account the confinement of the infilled concrete, is used to determine the material non-linearity of the infilled concrete.

Because the properties of the concrete inner plates are not equivalent to the inner spaces of the steel tubes, the hoop action of the concrete in the steel tube is not considered in the analysis of the concrete inner plates.

Nonlinear dynamic analysis is performed using the

Newmark method of direct integration. The time interval of the numerical integration is 1/400 sec. Rayleigh damping is employed and the damping constants of all members are assumed to 0.02. Two of the modes used for Rayleigh damping are the first and second out-of-plane modes.

The ground motions used in this analysis are based on the Design Specification for Highway Bridges 1996⁸⁾. They are standard strong earthquakes of Type I (T111, T112, T113) in conditions of stiff soil. The initial stress on the bridge is assumed to be the stress that is obtained under the dead-load condition^{16), 17)}.

When the bridge is subjected to a T113 earthquake in the out-of-plane direction, the maximum strains at the extreme edges of the steel tubes are as shown in Figure 4. The ordinate shows the strains on the steel tube and the abscissa is the coordinate in the longitudinal direction of the bridge. Element E101 (see Figure 5) of the R3 member at the springing part has the maximum strain. The maximum strain of the R2 member is observed in E110 near the joint between the arch rib and the floor system. For the R1 member, the largest strain is generated near lateral bracing K2 of the arch rib (the upper chord member E119 and the lower chord member E186). The strains of the lower chord members are larger than those of the upper chord members.

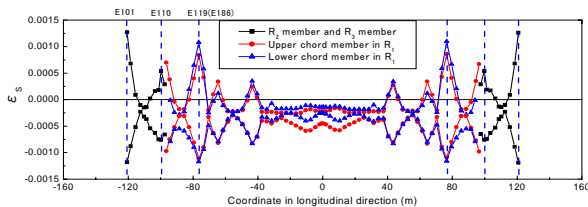
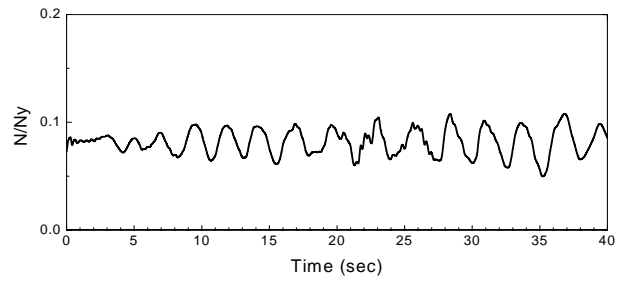


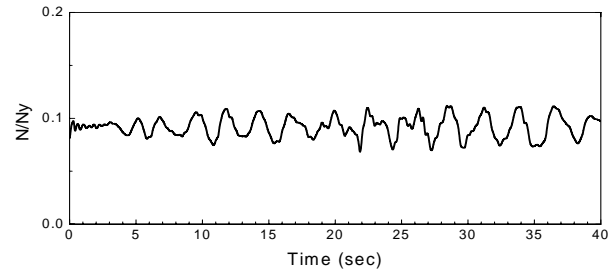
Figure 4 Maximum strains at the extreme edge of steel tubes

Time histories of the axial forces N are illustrated in Figure 5. Because the axial forces of the arch rib are essentially compressive forces, the yield compressive force N_y is used and the normalized axial force N/N_y is plotted along the vertical axis of the figure. Fluctuations in the axial forces are small since the maximum values are less than 10% of their yield compressive forces.

Time histories of the out-of-plane bending moment M_z and the in-plane bending moment M_y are shown in Figure 6.



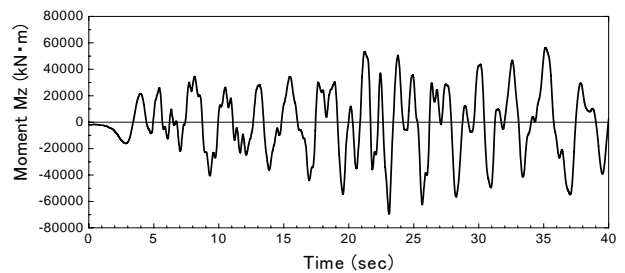
a) E101



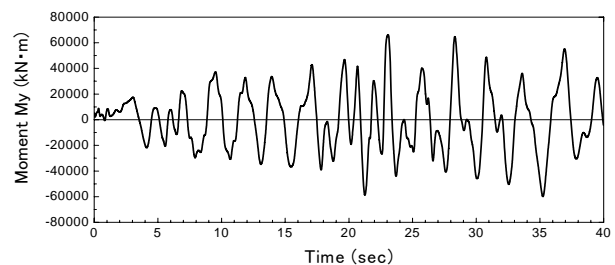
(b) E110

Figure 5 Time history of axial force

It is known that very large amounts of in-plane bending moment M_y of the arch rib are generated in addition to the out-of-plane bending moment M_z , even when the ground motion is applied in the out-of-plane direction. Because the in-plane and out-of-plane bending moments are greatly produced simultaneously, the analysis must consider the biaxial bending moment of the arch rib.



(a) Out-of-plane bending moment M_z



(b) In-plane bending moment M_y

Figure 6 Time history of bending moments in element E101

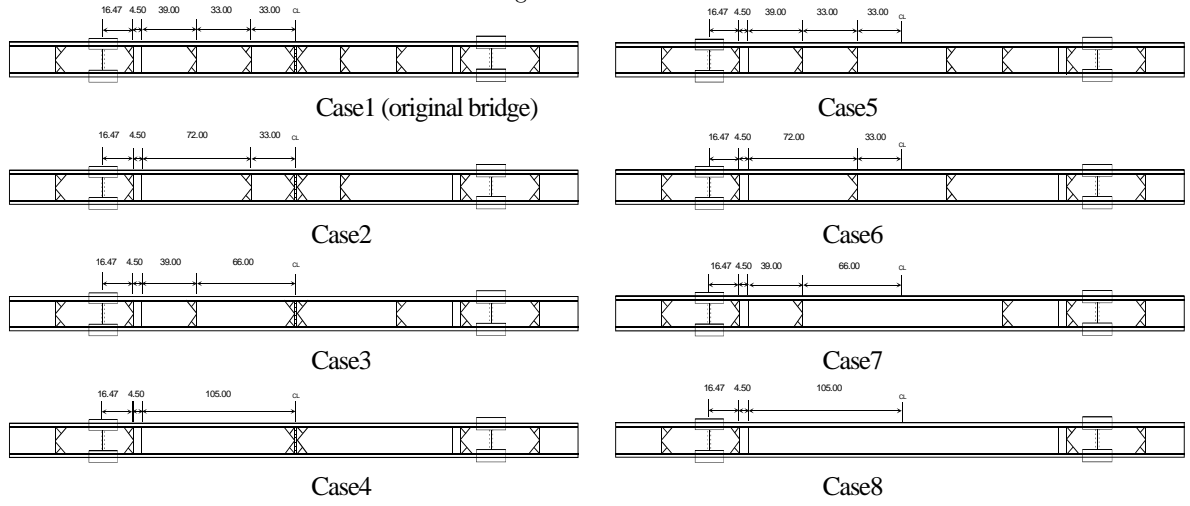


Figure 8 Arrangement patterns of lateral bracings

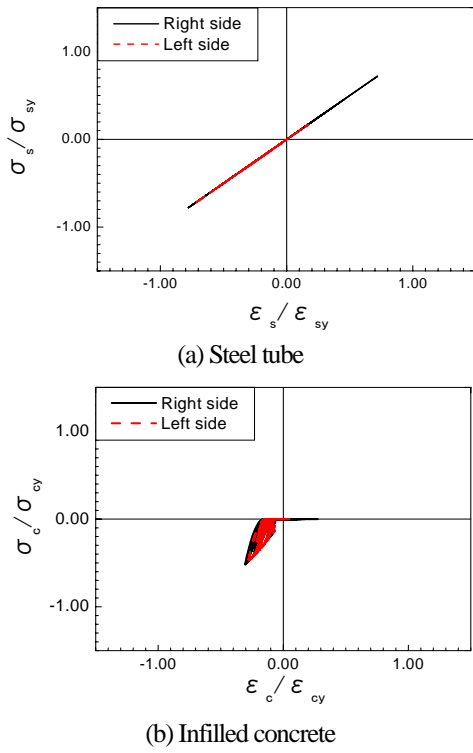


Figure 7 Stress-strain curves of steel tube and infilled concrete

Figure 7 demonstrates the stress-strain curves of the steel tube and the infilled concrete at the extreme edge. The vertical axis corresponds to the ratio of the stress (σ_s , σ_c) to the absolute value of the yield stress (σ_{sy} , σ_{cy}), and the longitudinal axis corresponds to the ratio of the strain (ϵ_s , ϵ_c) to the absolute value of the yield strain (ϵ_{sy} , ϵ_{cy}). The maximum strains in both the steel tubes and the infilled concrete do not reach the yield strain. Therefore, the arch rib of this CFT arch bridge is not damaged.

6. Effect of arrangement of lateral bracings in responses of CFT ribs

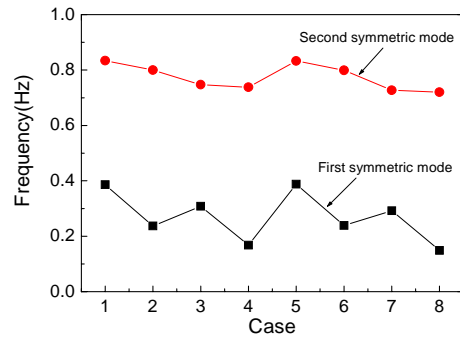
6.1 Analytical cases

The X-type, K2-type and K3-type lateral bracings for the arch rib in the main span are rearranged in present paper. Figure 8 shows the eight analytical models used in this paper. Case 1 corresponds to the actual bridge. Cases 2 through 4 are different combinations of X-type lateral bracings. Cases 5 through 7 are combinations without X-type lateral bracings. Case 8 corresponds to a model without those lateral bracings.

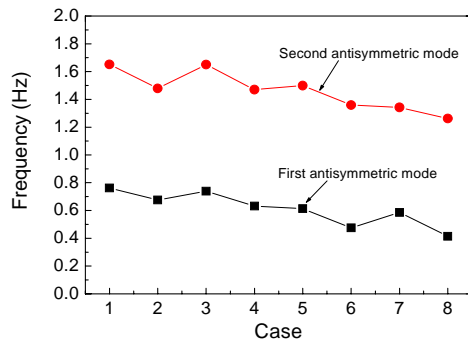
6.2 Effect of arrangement of lateral bracings on natural vibrations

The natural frequencies of the out-of-plane modes are sorted in Figure 9, according to the modal shapes of Case 1 (actual bridge, see Table 2). The arrangement of lateral bracings has such a small effect on the in-plane natural frequencies that the in-plane vibrations are not discussed in present paper.

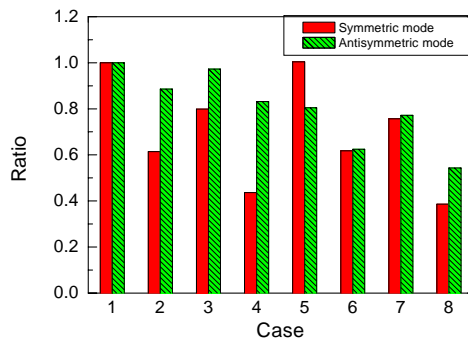
Figure 9(a) shows the first and second natural frequencies of the out-of-plane symmetrical modes. Comparing Cases 1, 3, 5 and 7, which have K2 lateral bracings, with Cases 2, 4, 6 and 8, which do not have K2 lateral bracings, the structure with K2 lateral bracings has higher natural frequencies than the structure without K2 lateral bracings. The effect of the X-type lateral bracing on the out-of-plane symmetrical modes is small because the frequencies of Case 5, which does not have X-type lateral bracing, is almost same as that of Case 1, which has X-type lateral bracing.



(a) Symmetric modes



(b) Antisymmetric modes



(c) Ratio

Figure 9 Natural frequencies of out-of-plane modes

Therefore, K2 lateral bracings have a large effect on the first out-of-plane symmetrical frequencies, while the X-type lateral bracing has a small effect on the first out-of-plane symmetrical frequencies.

The ratio between the frequencies of Case 2 through 8 and those of Case 1, which is constructed, is shown in Figure 9(c). The natural frequencies of the first out-of-plane symmetric modes are higher than those of Case 8, which has no lateral bracing. The natural frequencies of Cases 1 and 5, which have K2-type and K3-type lateral bracings, is 160% greater than that of Case 8, which has no lateral bracing.

Figure 9(b) shows the first and second natural

frequencies of the out-of-plane antisymmetric modes. X-type lateral bracing has an effect on the out-of-plane antisymmetric modes in all cases. Figure 13(c) shows that the first frequencies of the out-of-plane antisymmetric modes in Cases 1 and 3, which have

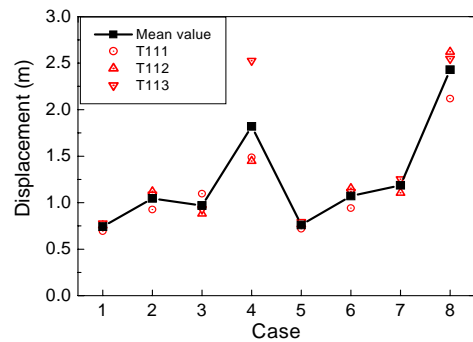
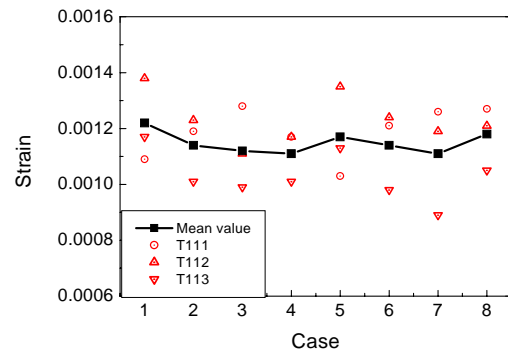


Figure 10 Out-of-plane displacements



(b) Lower chord member

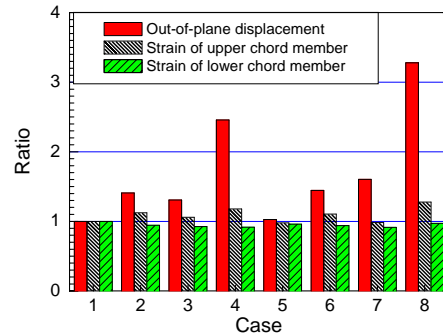


Figure 11 Strains of steel tube in R1 member

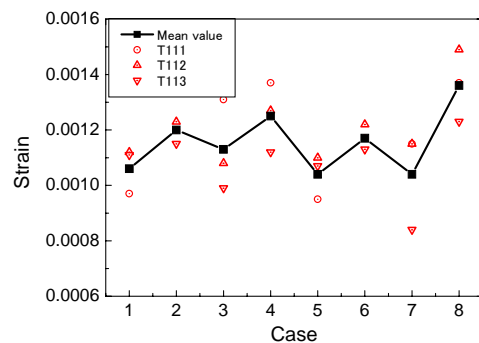


Figure 12 Ratio of maximum responses

(a) Upper chord member X-type lateral bracing, are 80% greater than that of Case 8, which has no lateral bracing.

The natural frequency of Case 5 that has no X-type bracing is smaller than that of Case 1, which has X-type bracing.

6.3 Effect of arrangement of lateral bracings on seismic responses of arch ribs

The effect of the arrangement of the lateral bracings on the seismic responses of arch ribs is also examined. The bridge is subjected to earthquake excitations in the out-of-plane direction. In general, the characteristics of the ground motions greatly influence the responses of bridge. Even when the ground motions have the same response spectrum, the bridge can have different responses. To solve this problem, this paper uses the mean value of the maximum responses for three strong ground motions, as recommended in Design Specifications for Highway Bridges 1996. The ground motions used in this analysis are the standard ground motions T111, T112 and T113.

Figures 10 and 11 show mean values of maximum out-of-plane displacements at the crown part of arch ribs, and maximum strains on R1 member respectively.

Figure 10 illustrates that the out-of-plane displacements of Case 1, which has X-type lateral bracing, and those of Case 5, which does not, are smaller than the displacements of the other cases. Therefore, the use of the K2-type and K3-type lateral bracings can decrease the seismic displacements of arch ribs. The effect of X-type lateral bracing on the seismic displacements of arch rib is small since the out-of-plane displacements in Cases 1 and 5 are of the same order.

Figure 11 shows that the change in the maximum strains generated in the upper chord members is greater than those in the lower chord members. The maximum strains in the upper chord members in Cases 1, 3, 5, and 7, which have K2-type lateral bracing, are smaller than those in the other cases. Therefore, K2-type lateral bracing can decrease the seismic responses of arch ribs.

The ratios of the responses of each case to those of Case 1 are shown in Figure 12. The out-of-plane displacements and the strains of the upper chord member in Case 5, which have K2-type and K3-type lateral bracings, are about 30% and 20% less than those in Case 8, which has no lateral bracing. Therefore, placing some lateral bracings near the quarter span of arch ribs seems to effectively decrease the seismic

responses of this CFT arch bridge when it is subjected to a uniform out-of-plane earthquake.

7. Conclusions

This paper evaluated the seismic response characteristics of a CFT arch bridge and the effect of the arrangement of lateral bracings on the seismic vibrations of the arch rib.

The main findings about the nonlinear seismic characteristics of this actual CFT arch bridge are as follows:

1. Biaxial bending moments should be considered in the seismic analysis of a CFT arch rib, because in-plane and out-of-plane bending moments are generated simultaneously when the bridge is subjected to an earthquake in the out-of-plane direction.
2. The fine performance of this CFT bridge is confirmed because the strains in arch ribs do not reach the yield strains.

What is worrying about CFT arch bridges is the increase in the out-of-plane responses of arch ribs when subjected to an out-of-plane ground motion. Placing some lateral bracings near the quarter span of arch ribs decreases the responses of the CFT arch ribs. The arrangement of lateral bracings has the following effects.

1. The natural frequencies of the out-of-plane symmetric modes for cases that have K-type lateral bracings near the quarter span of arch ribs is 160% larger than that those for cases that have no lateral bracing.
2. The natural frequencies of the out-of-plane antisymmetric modes for cases that have X-type lateral bracings in the half span of arch rib are 80% larger than those for cases that have no lateral bracing.
3. The out-of-plane displacements and the strains in the upper chord members that have K-type lateral bracings near the quarter span of arch ribs are about 30% and 20% less than those in the upper chord members that have no lateral bracing. The effect of arrangement of the lateral bracing decreases the seismic responses of CFT arch bridges.

References

- 1) Roeder C.W., Cameron, B. and Brown, C.B. : Composite action in concrete filled tubes. *Journal of Structural Engineering*, ASCE, 125(5), pp. 477-484, 1999.
- 2) Varma, A.H., Ricles, J.M., Sause, R. and Lu, L.W. : Experimental behavior of high strength square concrete-filled steel tube beam-columns. *Journal of Structural Engineering*, ASCE, 128(3), pp. 309-318, 2002.
- 3) Zhen, Z., Chen, B. and Wu, Q. : Recent development of CFST arch bridge in China, *Proceeding of 6th ASCCS Conference*, U.S.A., pp. 205-212. 2000.
- 4) Clawson, W.C. : Bridge applications of composite construction in the U.S., *Structural Engineering in the 21st Century, Proceedings of the 1999 Structures Congress*, pp. 544-547. 1999.
- 5) Nakamura, S. : New structural forms for steel/concrete composite bridges. *Structural Engineering International 1*, Journal of the International Association for Bridge and Structural Engineering (IABSE), pp. 45-50, 2000.
- 6) Wu, Q., Chen, B., Takahashi, K. and Nakamura, S. : Construction and technical subjects of concrete filled steel tubular arch bridges in China, *Bridge and Foundation Engineering*, 35(10), pp. 40-45. 2001(in Japanese).
- 7) Peng, D., Wu, Q., Takahashi, K. and Nakamura, S. : Recent construction and development of long-span bridges in China. *Bridge and Foundation Engineering*, 37(2), pp. 43-49. 2003 (in Japanese).
- 8) Earthquake Engineering Committee of Japan Society of Civil Engineers, : *Earthquake Resistant Design Codes in Japan*, Japan Society of Civil Engineering, Japan, 2000.
- 9) Japan Road Association : *Design Specifications for Highway Bridges*, Part V Seismic Design, 2002 (in Japanese).
- 10) Liu, Y., Hikosaka, H. and Chen, B.: Static characteristics and nonlinear seismic response of concrete-filled tubular arch bridge with half-though deck, *Steel Construction Engineering*, 23(6), pp. 53-61. 1999 (in Japanese).
- 11) Liu, Y., Hikosaka, H. and Chen, B.: Structural characteristic and seismic performance of steel-concrete composite tied arch bridge rigidly connected to piers, *Journal of Structural Engineering*, JSCE, 47A, pp. 1475-1484, 2001 (in Japanese).
- 12) Liu, Y. and Hikosaka, H. : Assessment for ultimate strength and seismic performance of braced-rib arch bridge using concrete-filled tubes, *Journal of Structure Mechanics and Earthquake Engineering*, JSCE, 703(I-59), pp. 313-325, 2002 (in Japanese).
- 13) Wu, Q., Takahashi, K., Matsuzaka, H., Chen, B. and Nakamura, S. : Study on dynamic properties of partially concrete filled steel tubular arch bridge, *Journal of Constructional Steel*, 10, pp. 141-148, 2002 (in Japanese).
- 14) Sato, T. : Confining mechanism and analytical model in circular concrete-filled steel tube under axial force, *Journal of Structure Construction Engineering*, 452, pp. 149-158, 1993(in Japanese).
- 15) Caughey, T.K. : Classical normal modes in damped linear dynamic systems, *Journal of Applied Mechanics* ASME, 27, pp. 269-271, 1960.
- 16) Ren, W.X. and Obata, M. : Elastic-plastic seismic behavior of long span cable-stayed bridges, *Journal of Bridge Engineering*, ASCE, 4(3), pp. 194-203, 1999.
- 17) Otsuka, H. : *Dynamic Design of Middle Span Bridges for Earthquake*, Kyushu University Press, Japan, 2000.
- 18) Wu, Q., Takahashi, K., Okabayashi, T. and Nakamura, S. : The effect of cable loosening on seismic response of a prestressed concrete cable-stayed bridge, *Journal of Sound and Vibration*, 268, pp. 71-84, 2003.